Performance of 3D Depth Migration Algorithms

Jan Thorbecke and Ben Geesink

Thursday June 10 1999;
Presentations: 9:20, 9:45, 10:10

Slide 1

sgi

Extrapolation techniques discussed

- 2-dimensional convolution, Blacquière et al. (1989)
- Hale-McClellan recursion, Hale (1991)
- series expansion in $\cos(kr)$ Thorbecke (1997)
- phase screen Stoffa et al. (1990)
- finite-difference Li (1991)

Every method is explained briefly and implementation details of the algorithms are discussed. Numerical examples are given for impulse responses. Finally, we demonstrate how each of the algorithms can benefit from the use of multiple processors.

Slide 2

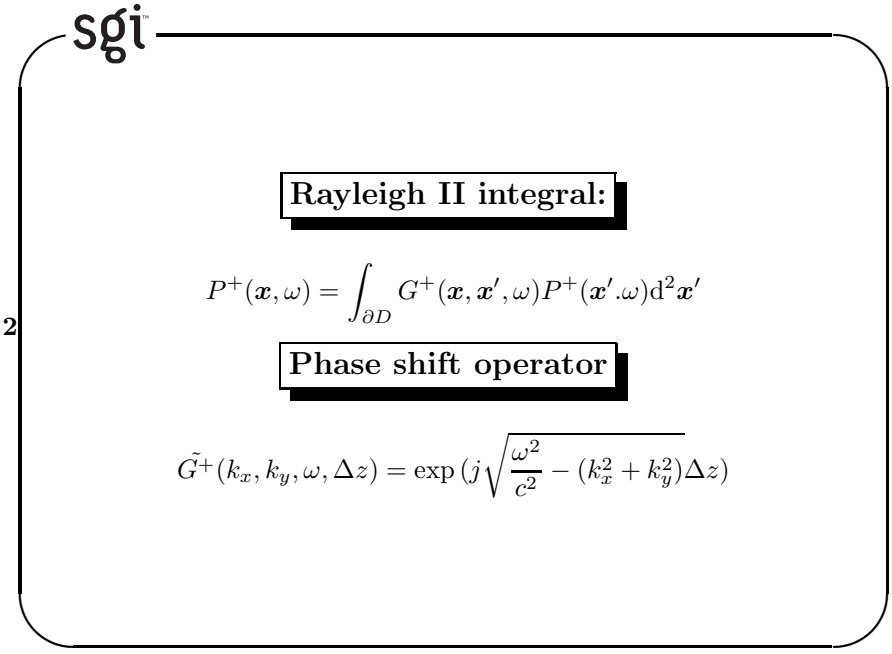

where $P^+(\boldsymbol{x}',\omega)$ represents the measured wave field at the surface ∂D and $G^+(\boldsymbol{x},\boldsymbol{x}',\omega)$ represents the extrapolation operator (Greens function) from the surface ∂D to a point in the subsurface $\boldsymbol{x}$ **?**.

In homogeneous media the one-way extrapolation operator in the $\boldsymbol{k}-\omega$ (wavenumber-frequency) domain is a simple analytical function which is given by **?**:

$$\tilde{G}(k_x,k_y,\omega,\Delta z) = \exp\left(j\sqrt{\frac{\omega^2}{c^2} - (k_x^2+k_y^2)}\Delta z\right) \tag{1}$$

with Δz being a small extrapolation step and c the propagation velocity of the medium. The advantage of using the phase shift operator in the $k_x, k_y - \omega$ domain is that the extrapolation result is obtained by multiplication of the data with the phase shift operator. However, multiplication in the $k_x, k_y - \omega$ domain rules out the possibility of applying a laterally varying operator. To allow laterally varying medium functions a convolution operator in the $x, y - \omega$ (space-frequency) domain should be used. This spatial convolution operator must be designed in such a way that it gives accurate and stable results within a reasonable computational time. To arrive at this goal two steps must be taken; the first step is an optimum *design* of the spatial operator and the second step deals with a fast *implementation* of the spatial convolution. The most efficient algorithms combine these two steps and a spatial operator is designed in such a way that it can be implemented in a fast way. Note that the extrapolation operator is circular symmetric which makes an efficient optimization and implementation possible.

Slide 3

sgi

Approximations to the phase-shift operator

$$\tilde{G}(k_x, k_y) = \exp(jk_z\Delta z)$$
$$\approx \sum_{m=0}^{M}\sum_{n=0}^{N} G_{mn}\cos(k_x m\Delta x)\cos(k_y n\Delta y)$$
$$\approx \sum_{l=0}^{L} G_l T_l(\cos(k_r\Delta x))$$
$$\approx \sum_{j=0}^{J} Y_j[\cos(k_r\Delta x)]^j$$

Most spatial extrapolation methods can be expressed in the wavenumber domain as an approximation to the phase shift operator of equation (1). Different approximations can be based on a power series or on an expansion with respect to the cosine terms of the Fourier transform. Transforming these expansions, with a limited number of terms and in an optimal way, to the spatial domain gives the spatial convolution operator. Three types of expansions are discussed:

$$\tilde{G}(k_x, k_y) = \exp(jk_z\Delta z)$$
$$\approx \sum_{m=0}^{M}\sum_{n=0}^{N} G_{mn}\cos(k_x m\Delta x)\cos(k_y n\Delta y) \quad (2)$$
$$\approx \sum_{l=0}^{L} G_l T_l(\cos(k_r\Delta x)) \quad (3)$$
$$\approx \sum_{j=0}^{J} Y_j[\cos(k_r\Delta x)]^j \quad (4)$$

with $k_r = \sqrt{(k_x^2 + k_y^2)}$ and $k_z = \sqrt{k^2 - k_r^2}$. Note that there are many more expansions possible like the expansions in Laplacian $(k_x^2 + k_y^2)$**?** or k_z terms.

Equation (2) represents the inverse Fourier transform of a symmetric (in x and y) spatially limited operator. G_{mn} are the coefficients of the 2-D spatial convolution operator. The coefficients G_{mn} used in this paper are obtained by a Weighted Least Squares optimization method. The spatial dimensions of the convolution operator are $(2M-1)^2$).

In equation (3) the 2-dimensional problem is reduced to a 1-dimensional filter problem using the circular symmetry of the 2-D phase shift operator Hale (1991). This method is represented by an Chebychev polynomial (T_l) in 1-dimensional cosine terms. The coefficients G_l represent the 1-D phase-shift operator and are obtained with any preferred 1-D

optimization method. The cosine terms $\cos(k_r \Delta x)$ are approximated by small (SxS) 2-D convolution filters. The spatial size of the operator is $(L(S-1)-S+2)^2$.

Equation (4) is a series expansions in $\cos(k_r \Delta x)$. The cosine terms are approximated by small (SxS) 2-D convolution filters. The coefficients Y_j in the series expansions are obtained by numerically optimizing the coefficients given the approximation of the cosine terms. Note that the number of expansion terms is more limited by the accuracy of the floating point implementation than the Chebychev recursion. The spatial size of the operator is also $(J(S-1)-S+2)^2$.

Slide 4

sgi

Approximations to the one-way wave equation

$$\frac{\partial P(\boldsymbol{x},\omega)}{\partial z} \approx j\sqrt{\frac{\omega}{c(\boldsymbol{x})}+\frac{\partial^2}{\partial x^2}+\frac{\partial^2}{\partial y^2}}P(\boldsymbol{x},\omega)$$

$$\approx j\frac{\omega}{c(\boldsymbol{x})}\left[1+\sum_{i=1}^{n}\frac{\alpha_i S_x}{1+\beta_i S_x}+\sum_{i=1}^{n}\frac{\alpha_i S_y}{1+\beta_i S_y}P(\boldsymbol{x},\omega)\right]$$

$$S_x = \frac{c^2(\boldsymbol{x})}{\omega^2}\frac{\partial^2}{\partial x^2}, S_y = \frac{c^2(\boldsymbol{x})}{\omega^2}\frac{\partial^2}{\partial y^2}$$

$$P(\boldsymbol{x}, z+dz, \omega) \approx exp(jk(\frac{\bar{c}}{c(\boldsymbol{x})}-1)\Delta z)FT_{\boldsymbol{k}}\left[exp(jk_z\Delta z)\tilde{P}(\boldsymbol{k},z,\omega)\right]$$

Slide 5

Impulse response (25x25)

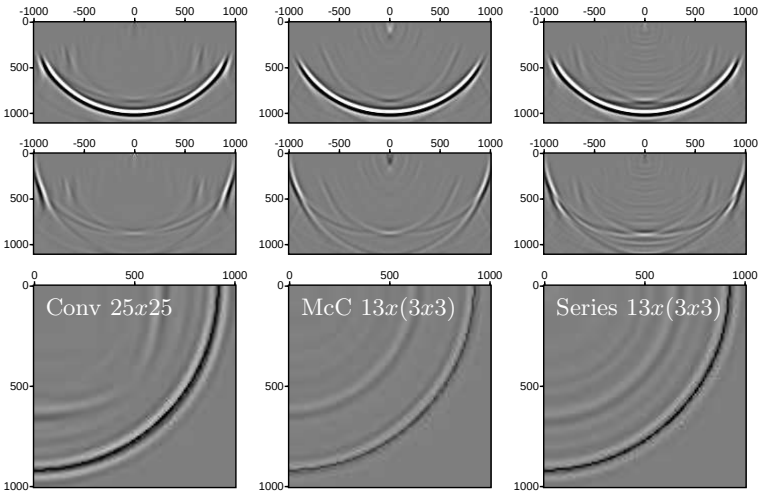

Slide 6

Impulse response (33x33)

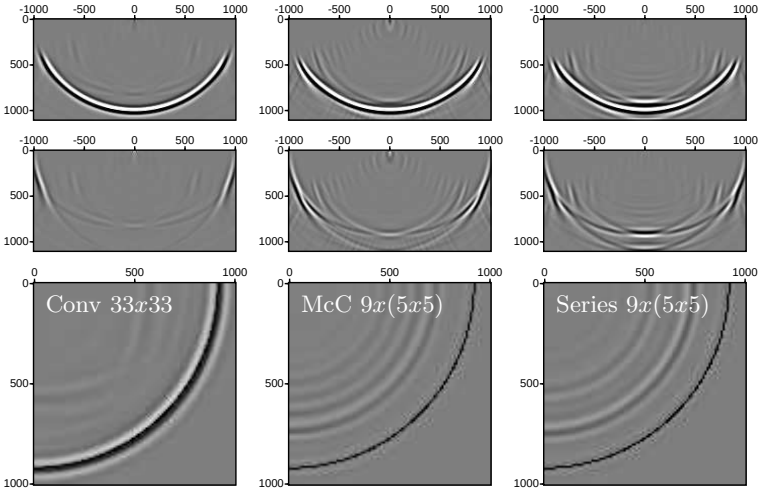

Slide 7

Impulse response (21x21+13x(5x5))

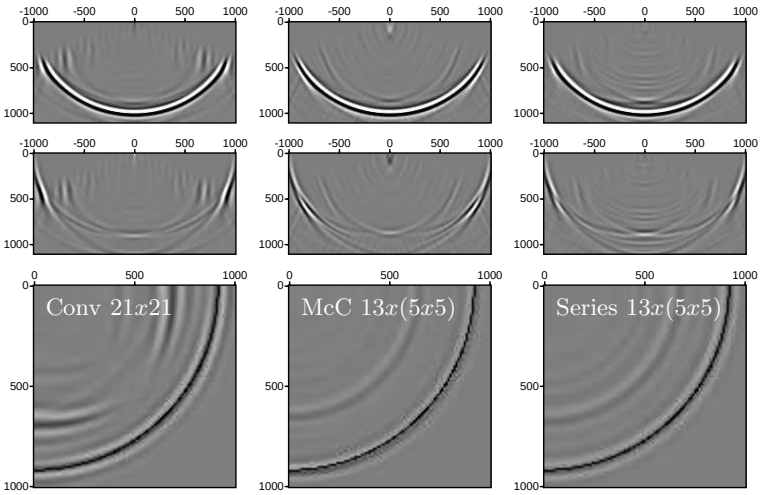

Slide 8

Impulse response

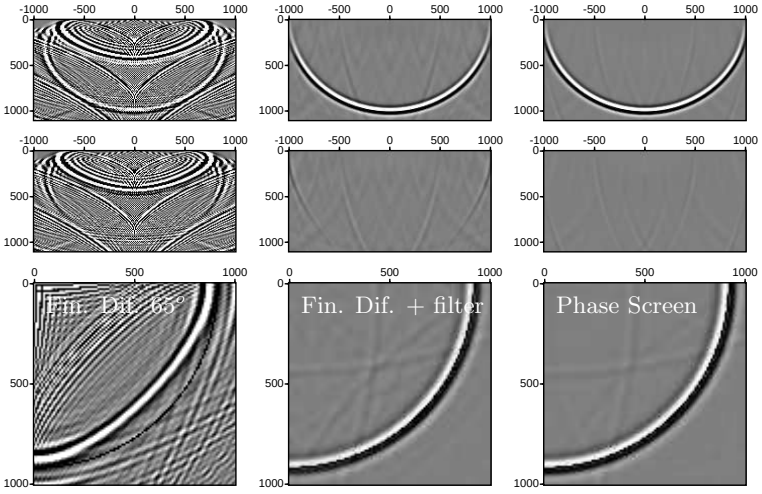

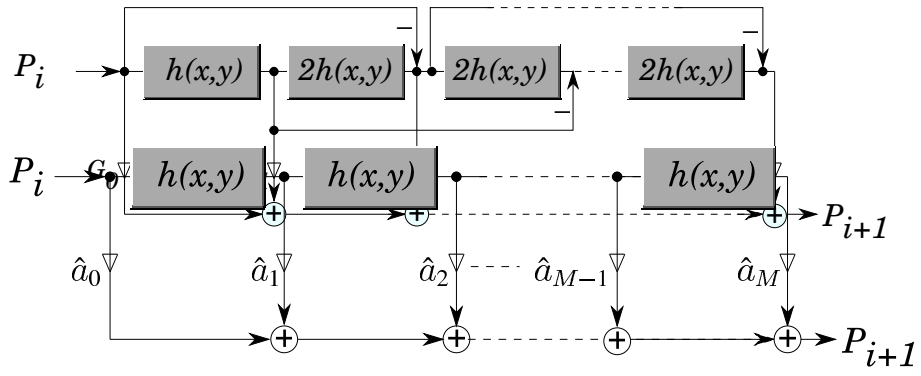

To check the accuracy of the extrapolation method an impulse response is calculated with $\Delta x = \Delta y = \Delta z = 10$ m, $c = 1000m/s$ and a Ricker wavelet with a time delay of 1.0 seconds and a frequency peak at 10 Hz. The impulse response shows us three things; the circularity of the operator, the numerical artifacts and the result at high angles.

To have a fair comparison between the different methods the footprint of the spatial operator is chosen to be the same. For the 2D convolution we have used a 33x33 convolution operator and for the Chebychev recursion and series expansion we used a 3x3 operator for the cosine operator and 17 terms in the expansion. In Figure **??** the impulse responses are shown for the three spatial convolution methods. Note that all methods give comparable results; the depth slice at 67^o of the 2D convolution shows a higher (more accurate) amplitude than the other methods. Note that a higher accuracy for the cosine methods can be achieved by optimizing the cosine terms for every wavenumber $k = \frac{\omega}{c}$. However, the performance will suffer from the fact that the cos(kr) stencil depends on the local velocity. Using a larger stencil (5x5) and less terms (9,) to have the same footprint, gives non-accurate results. A 13x(5x5) operator gives comparable results but has a much larger footprint.

In recursive depth extrapolation the (complex) computations are carried out from the xy plane at depth z to the xy plane at depth $z + \Delta z$. The secondary cache of the MIPS R10k, which is used in the Origin 2000, has a size of 4 MB and can contain one xy plane (of complex numbers) of 724×724 samples or 2 planes of 512×512. Larger or more depth planes will cause cache misses and introduces a higher latency on load/store operations. The R10K has 32 64-bit floating point registers and can do one multiply-add and one load/store operations at every clock-cycle. Taking these hardware constraints into account the implementation of the different extrapolation methods was carried out:

- The implementation of the 2D spatial convolution operators uses the symmetry in x and y explicitly. To reduce misses from the cache the data is rearranged in such a way that the convolution can be done within the cache.

```
for (iy = 0; iy < ny; iy++) {
    for (ix = 0; ix < nx; ix++) {
        for (j = 0; j < opersize; j++) {
            data[iy*nx+ix] += (tmp3[index3+j] + tmp4[index4+j])*hopx[j];
}   }   }
```

- The Hale McClellan method is implemented as a Chebychev recursion scheme as shown in Figure **??**. The recursion scheme is not very cache friendly because three copies of the xy planes are needed to calculate the plane at $z + \Delta z$. The basic scheme is given by:

```
for (o = 0; o < order; o++)
    for (iy = 0; iy < ny; iy++)
        for (ix = 0; ix < nx; ix++)
            term3[iy*nx+ix]  = 2.0*term2[iy*nx+ix] - term1[iy*nx+ix];
            data[iy*nx+ix] += op[o]*term3[iy*nx+ix];
}   }   }
```

  Note that all arrays in these calculations are complex. The term[1,2,3] arrays contain the pre-computed results of the small 2D convolutions of $\cos(k_r \Delta x)$ at different orders.

- The series expansion in $\cos(k_r \Delta x)$, also shown in Figure **??**, is a straightforward implementation of the small 2D convolutions without the extra storage as needed in the Chebychev recursion scheme.

```
for (o = 0; o < order; o++) {
    for (iy = 0; iy < nyo; iy++) {
        for (ix = 0; ix < nxo; ix++) {
            data[iy*nx+ix] += a_m[o]*term1[iy*nx+ix];
}   }   }
```

Slide 9

2D-Convolution

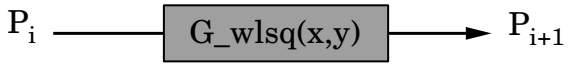


```
for (iy = 0; iy < ny; iy++) {
    for (ix = 0; ix < nx; ix++) {
        for (j = 0; j < opersize; j++) {
            data[iy*nx+ix] += (tmp3[index3+j] + tmp4[index4+j])*hopx[j];
}   }   }
```

Slide 10

Hale McClellan

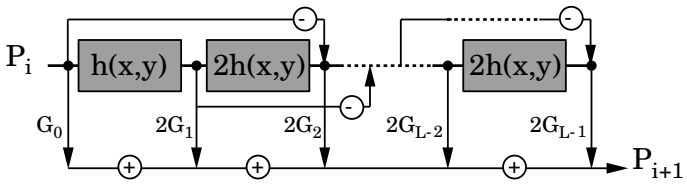


```
for (o = 0; o < order; o++) {
    for (iy = 0; iy < ny; iy++) {
        for (ix = 0; ix < nx; ix++) {
            term3[iy*nx+ix]  = 2.0*term2[iy*nx+ix] - term1[iy*nx+ix];
            data[iy*nx+ix] += op[o]*term3[iy*nx+ix];
}   }   }
```

Slide 11

Series

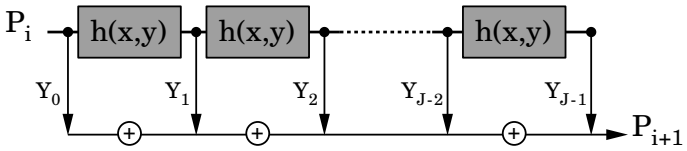


```
for (o = 0; o < order; o++) {
    for (iy = 0; iy < nyo; iy++) {
        for (ix = 0; ix < nxo; ix++) {
            data[iy*nx+ix] += a_m[o]*term1[iy*nx+ix];
}   }   }
```

Slide 12

Phase-Screen

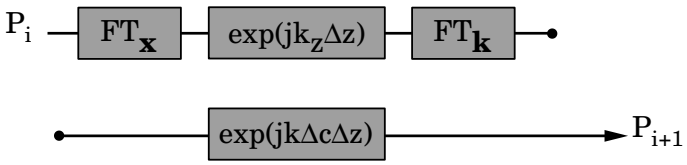

$\Delta c = 1/c(x,y,z)-1/c(z)$

Slide 13

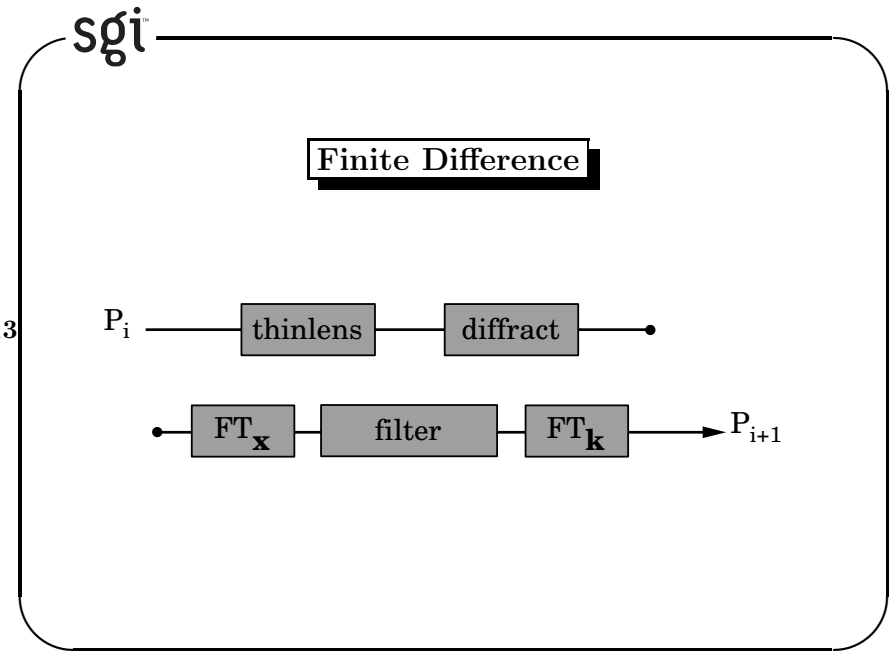

The table above shows the kind and number of operations for every (x, y) point in the xy plane of the most inner-loop in the convolution. From this table it can be concluded that the 2D convolution is bound by the number of load/store operations. Note that it is possible to implement the 2D convolution in such a way (by not using the symmetry in the operator) that it will be floating point bound. Although this code will run closer to maximum performance, it will also use more operations and it will take more time for the same task. The Hale McClellan scheme is also bound by the number of load/store operations and can only be run at 50% of the floating point peak performance. The series expansion is the only scheme which is bound by the number of floating point operations.

In the migration the extrapolation takes 95 % of the total migration time. The other 5% is taken by the computation of the operator table and IO. In the table below the number of flops are shown for the impulse response calculation for the different methods:

Slide 14

sgi

Results small model on R10K 195 MHz

model size: $201 * 201 * 111 (nx * ny * nz)$

Method	Size	table (s)	migr (s)	misc (s)	tot (s)	Mf/s
Conv	25x25	286.3	2104.5	0.7	2391.5	-
McC	13x(3x3)	0.1	946.2	0.7	946.9	-
Series	13x(3x3)	44.6	802.5	0.7	847.8	-
Conv	33x33	625.0	3480.7	0.7	4106.4	-
McC	9x(5x5)	0.1	906.1	0.7	906.9	-
Series	9x(5x5)	30.6	812.1	0.6	843.3	-
PSPC	-	0.0	532.3	0.7	533.0	-
FinDif	-	0.0	672.3	0.7	673.0	-

Slide 15

sgi

Results medium model on R10K 195 MHz

model size: $2001 * 1201 * 7 (nx * ny * nz)$

Method	Size	table (s)	migr (s)	misc (s)	tot (s)	Mf/s
Conv	25x25	293.3	7786.9	13.1	8093.3	-
McC	13x(3x3)	0.1	5172.4	12.5	5185.0	-
Series	13x(3x3)	218.4	4313.9	12.9	4545.2	-
Conv	33x33	640.7	11971.	12.8	12625.	-
McC	9x(5x5)	0.1	4454.6	12.6	4467.3	-
Series	9x(5x5)	142.9	3852.7	12.6	4008.2	-
PSPC	-	0.0	2324.1	13.0	2337.1	-
FinDif	-	0.0	3594.5	14.8	3609.3	-

Slide 16

Compare single CPU: R10K 195, 250 + R12K 300 MHz

model size: $2001 * 1201 * 7(nx * ny * nz)$

Slide 17

		small			medium		
Method	Size	195	250	300 (vs250)	195	250	300 (vs250)
Conv	25x25	1.0	1.40	1.65 (1.18)	1.0	1.27	1.65 (1.29)
McC	13x(3x3)	1.0	1.35	1.76 (1.30)	1.0	1.54	1.26 (0.82)
Series	13x(3x3)	1.0	1.37	1.74 (1.26)	1.0	1.52	1.31 (0.86)
Conv	33x33	1.0	1.43	1.65 (1.15)	1.0	1.25	1.64 (1.31)
McC	9x(5x5)	1.0	1.33	1.71 (1.28)	1.0	1.29	1.33 (1.03)
Series	9x(5x5)	1.0	1.29	1.74 (1.34)	1.0	1.44	1.43 (1.00)
PSPC	-	1.0	1.28	1.67 (1.30)	1.0	1.23	1.47 (1.19)
FinDif	-	1.0	1.42	1.81 (1.27)	1.0	1.31	1.50 (1.14)

Slide 18

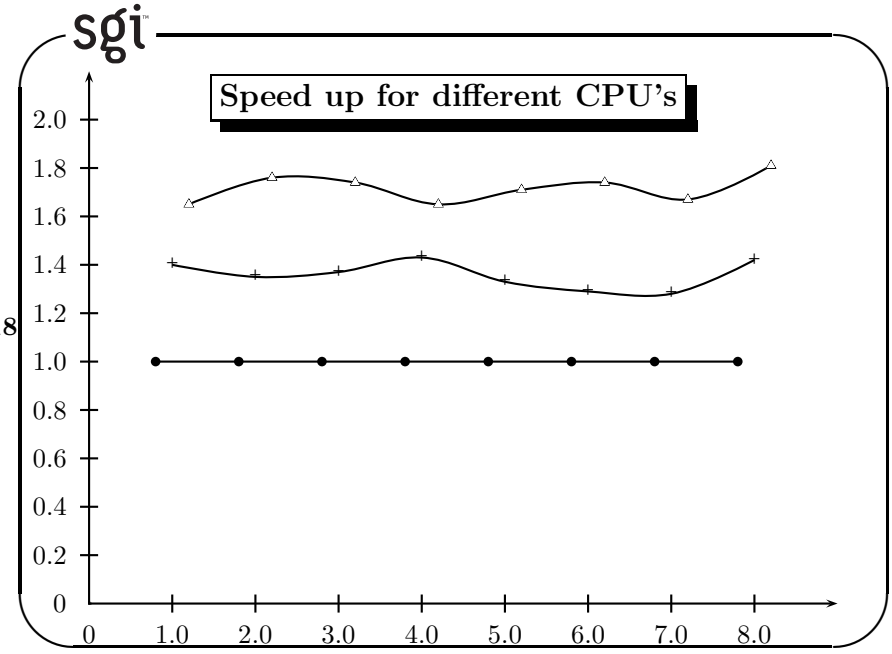

Slide 19

Results small model on R10K 250 MHz

model size: $201 * 201 * 111 (nx * ny * nz)$

Method	Size	table (s)	migr (s)	misc (s)	tot (s)	Mf/s
Conv	25x25	115.5	1596.9	0.7	1713.1	290
McC	13x(3x3)	0.1	699.9	0.6	700.7	165
Series	13x(3x3)	33.2	581.7	0.7	615.6	200
Conv	33x33	253.8	2612.3	2.2	2868.3	305
McC	9x(5x5)	0.1	680.2	0.7	681.0	180
Series	9x(5x5)	22.9	630.9	0.6	654.4	190
PSPC	-	0.0	414.8	0.6	415.4	175
FinDif	-	0.0	471.1	0.6	471.7	200

```
nxv=201 dxv=10 nyv=201 dyv=10 nzv=11 dzv=10 fmin=5 fmax=5 dstep=10
                      cycles       flops    seconds
Conv   25x25       1389070136  1659536661     2.293
McC    13x(3x3)     257262027   181424747     1.040
Series 13x(3x3)     489700519   371343254     0.818
Conv   33x33       2647420950  3466367284     3.733
McC    9x(5x5)      241696370   192538144     1.016
Series 9x(5x5)      413381696   313259119     0.918
Phase screen        155578346   108577671     0.595
Finite Difference   159197841   148239311     0.715

nxv=201 dxv=10 nyv=201 dyv=10 nzv=21 dzv=10 fmin=5 fmax=5 dtsep=20
                      cycles        flops       seconds
Conv   25x25        2031708960  2358601265
McC    13x(3x3)      509045729   362559134
Series 13x(3x3)      700171619   543454491
Conv   33x33        3698230648  4654437895
McC    9x(5x5)       477980469   384835411
Series 9x(5x5)       631730703   494245936
Phase screen         305982404   217037153
Finite Difference    313223405   296360433
                    nz=10 nw=1
                   flops migr     flops table     MF/s
Conv   25x25        699064604     960472057      291
McC    13x(3x3)     181134387        290360      166
Series 13x(3x3)     172111237     199232017      200
Conv   33x33       1188070611    2278296673      303
McC    9x(5x5)      192297267        240877      181
Series 9x(5x5)      180986817     132272302      188
Phase screen        108459482        118189      173
Finite Difference   148121122        118189      197
```

Slide 20

Parallel results small model on R10K 250 MHz

model size: $201 * 201 * 111 (nx * ny * nz)$

CPU's	table (s)	migr (s)	comm (s)	tot (s)	scaling
1	115.5	1596.9	0.2	1713.1	1.00
2	58.0	801.2	0.5	860.2	1.99
4	29.3	400.9	2.2	433.0	3.96
8	15.6	198.3	2.4	216.8	7.90
16	8.8	101.9	2.3	113.7	15.0
32	5.5	51.4	2.8	60.5	28.3

Slide 21

Results medium model on R10K 250 MHz

model size: $2001 * 1201 * 7 (nx * ny * nz)$

Method	Size	table (s)	migr (s)	misc (s)	tot (s)	Mf/s
Conv	25x25	448.6	5889.4	13.7	6351.7	260
McC	13x(3x3)	0.1	3360.0	14.2	3374.3	110
Series	13x(3x3)	166.4	2789.1	18.6	2974.1	125
Conv	33x33	972.2	9096.2	13.4	10082	285
McC	9x(5x5)	0.1	3447.2	13.6	3460.9	130
Series	9x(5x5)	111.9	2643.3	14.4	2769.6	140
PSPC	-	0.0	1871.4	22.3	1893.7	130
FinDif	-	0.0	2735.2	18.7	2753.9	135

```
nxv=2001 dxv=10 nyv=1201 dyv=10 nzv=2 dzv=10 fmin=5 fmax=5
                      cycles       flops    seconds
Conv   25x25        6474333504   7922247490
McC    13x(3x3)     1497153863   1065195911
Series 13x(3x3)     2554199170   1844055181
Conv   33x33       11966326268  15938236438
McC    9x(5x5)      1370365146   1137305603
Series 9x(5x5)      2170610967   1625743155
Phase screen         784997848    609343983
Finite Difference   944664815     961634138

nxv=2001 dxv=10 nyv=1201 dyv=10 nzv=3 dzv=10 fmin=5 fmax=5
                      cycles       flops    seconds
Conv   25x25       10257457988  12071459860
McC    13x(3x3)     2967973902   2125267290
Series 13x(3x3)     3804178606   2851069970
Conv   33x33       18150526816  22991455023
McC    9x(5x5)      2714435379   2269537798
Series 9x(5x5)      3450707766   2690518819
Phase screen        1543911914   1213735299
Finite Difference   1863245629   1918315609

                    nz=1 nw=1
                   flops migr  seconds   MF/s
Conv   25x25       4149212370   15.291    258
McC    13x(3x3)    1060071379    9.363    108
Series 13x(3x3)    1007014789    7.646    125
Conv   33x33       7053218585   23.705    284
McC    9x(5x5)     1132232195    8.166    132
Series 9x(5x5)     1064775664    7.327    139
Phase screen        604391316    4.416    130
Finite Difference   956681471    6.823    133
```

Slide 22

Parallel results medium model on R10K 250 MHz

model size: $2001 * 1201 * 7 (nx * ny * nz)$ for Convolution (25x25)

CPU's	table (s)	migr (s)	comm (s)	tot (s)	scaling
1	448.6	5889.4	11.8	6351.7	1.00
2	229.6	2979.6	34.1	3247.0	1.96
4	117.7	1486.4	12.1	1618.1	3.93
8	63.9	749.4	37.7	853.9	7.44
16	34.3	378.3	26.2	440.9	14.4
32	19.6	196.1	31.3	249.2	25.5

Slide 23

Speed up for R10K250 MHz

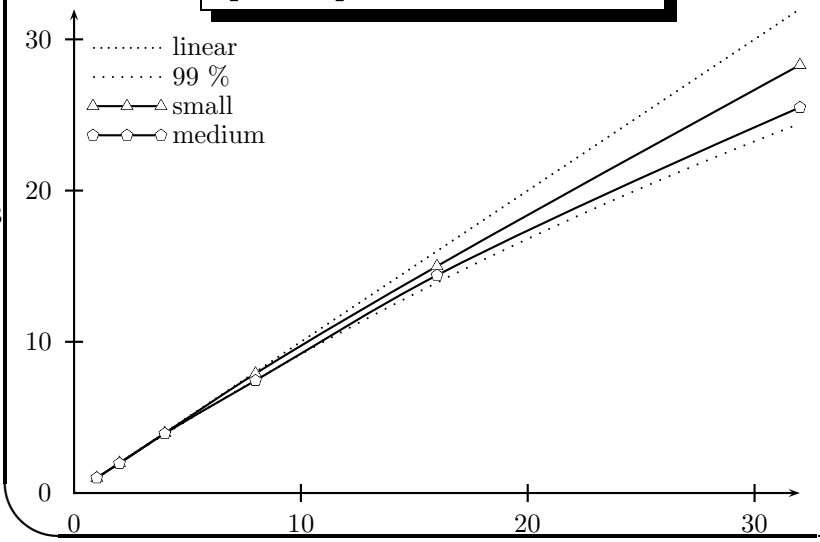

Slide 24

sgi

Results small model on R12K 300 MHz

model size: $201 * 201 * 111 (nx * ny * nz)$

Method	Size	table (s)	migr (s)	misc (s)	tot (s)	Mf/s
Conv	25x25	173.3	1270.8	0.8	1444.9	365
McC	13x(3x3)	0.1	537.3	0.7	538.1	260
Series	13x(3x3)	26.5	460.5	0.7	487.7	245
Conv	33x33	394.3	2087.4	0.8	2482.5	385
McC	9x(5x5)	0.1	529.9	0.7	530.7	225
Series	9x(5x5)	18.1	466.0	0.7	484.8	251
PSPC	-	0.0	317.7	0.7	318.4	200
FinDif	-	0.0	370.0	1.0	371.0	245

nz=10 nw=1 flops migr time Conv 25x25 699064604 1.816 McC 13x(3x3) 181134387 0.668 Series 13x(3x3) 172111237 0.675 Conv 33x33 1188070611 2.943 McC 9x(5x5) 192297267 0.816 Series 9x(5x5) 180986817 0.687 Phase screen 108459482 0.515 Finite Difference 148121122 0.577

Slide 25

Parallel results small model on R12K 300 MHz

model size: $201 * 201 * 111 (nx * ny * nz)$

CPU's	table (s)	migr (s)	comm (s)	tot (s)	scaling
1	173.3	1270.8	0.0	1444.9	1.00
2	87.1	634.7	0.5	723.2	2.00
4	44.5	319.4	1.5	366.4	3.94
8	22.8	162.0	2.7	188.4	7.67
16	12.2	82.6	3.5	99.3	14.6
32	7.9	47.1	5.2	61.7	23.4
64	8.2	23.4	5.8	39.4	36.7

Slide 26

Results medium model on R12K 300 MHz

model size: $2001 * 1201 * 7 (nx * ny * nz)$

Method	Size	table (s)	migr (s)	misc (s)	tot (s)	Mf/s
Conv	25x25	175.4	4718.7	12.6	4905.7	325
McC	13x(3x3)	0.1	4094.4	17.9	4112.4	120
Series	13x(3x3)	140.9	3303.4	13.4	3457.7	140
Conv	33x33	403.0	7261.2	13.8	7678.0	360
McC	9x(5x5)	0.1	3333.8	18.4	3352.3	150
Series	9x(5x5)	84.2	2678.4	15.0	2777.6	165
PSPC	-	0.0	1567.3	15.4	1582.7	150
FinDif	-	0.0	2383.9	13.3	2397.2	155

nz=1 nw=1 flops migr seconds MF/s Conv 25x25 4149212370 12.158 325 McC 13x(3x3) 1060071379 8.300 122 Series 13x(3x3) 1007014789 6.951 138 Conv 33x33 7053218585 18.570 362 McC 9x(5x5) 1132232195 7.162 151 Series 9x(5x5) 1064775664 6.158 165 Phase screen 604391316 3.903 148 Finite Difference 956681471 5.796 157

Slide 27

sgi

Parallel results medium model on R12K 300 MHz

model size: $2001 * 1201 * 7(nx * ny * nz)$ for Convolution (25x25)

CPU's	table (s)	migr (s)	comm (s)	tot (s)	scaling
1	175.4	4718.7	0.0	4905.7	1.00
2	87.6	2376.2	2.1	2481.8	1.98
4	45.3	1212.6	5.0	1282.2	3.82
8	23.2	602.7	6.9	642.5	7.63
16	11.7	310.6	9.9	345.9	14.2
32	7.0	167.9	13.9	203.8	24.1
64	6.5	101.1	17.3	139.5	35.2

Slide 28

Speed up for R12K 300 MHz

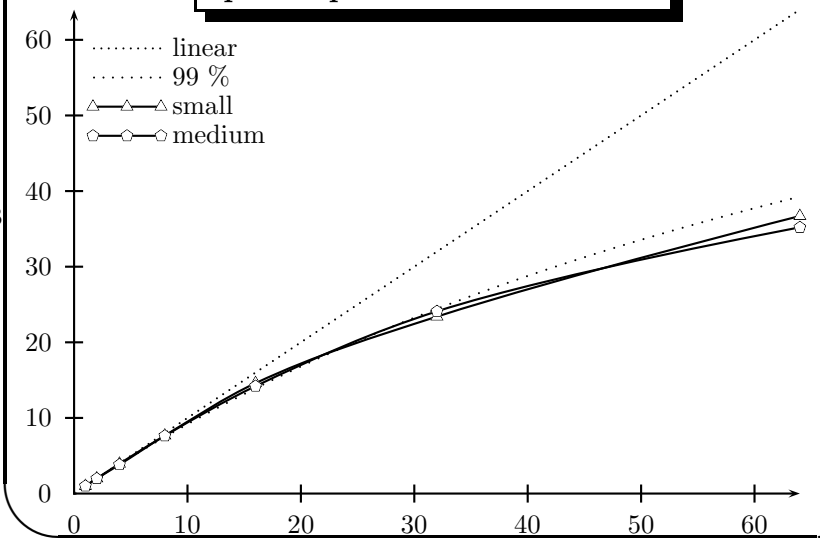

Slide 29

Detailed scaling for R12K 300 MHz

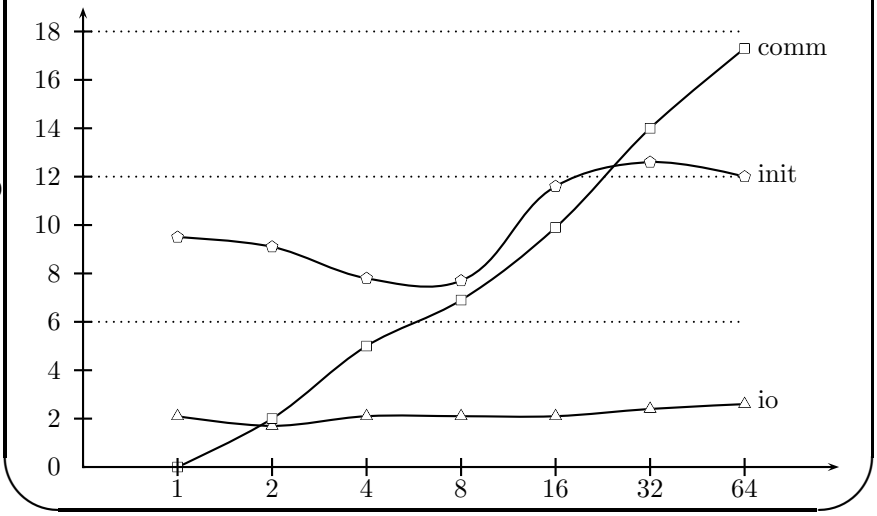

Slide 30

sgi

Comparison

method	accuracy	circular	table	impl	perf
Conv (33x33)	+	+	-	++	□
Conv (25x25)	+	+	□	++	+
McC 13x(3x3)	□/+	□	+	□	□
McC 9x(5x5)	-	□	++	□	□/+
Series 13x(3x3)	□/+	□/+	□	++	++
Series 9x(5x5)	-	□	+	++	++
PSPC	++	++	++	++	+
FinDif	++	+	++	+	+

Note; accuracy is defined in homogeneous medium.

In the table below a simplified summary is given. The columns in this table have the following meaning:
• *circular*: the circularity of the impulse response.
• *table*: the amount of cycles needed to compute all the operator coefficients needed in the convolution scheme. In the table ++ means a minimum time.
• *implementation*: the simplicity of the implementation.
• *performance*: the performance of the scheme on the Origin 2000.

Slide 31

Conclusions

- the 2D convolution requires the most multiplications and additions but also makes best use of the hardware
- the performance of the Hale McClellan method suffers from the extra copy needed in the Chebychev recursion scheme
- the series expansion overcomes this problem and can be implemented more efficiently
- PSPC and Finite Difference needs to be tested in inhomogeneous model

Slide 32

References

Blacquière, G., Debeye, H. W. J., Wapenaar, C. P. A., and Berkhout, A. J., 1989, 3D table-driven migration: Geophysical Prospecting, **37**, no. 8, 925–958.

Hale, D., 1991, 3-D depth migration via McClellan transformations: Geophysics, **56**, 1778–1785.

Li, Z., 1991, Compensating finite-difference errors in 3-D migration and modeling: Geophysics, **56**, 1650–1660.

Stoffa, P. L., Fokkema, J. T., de Luna Freire, R. M., and Kessinger, W. P., 1990, Split-step fourier migration: Geophysics, **55**, no. 04, 410–421.

Thorbecke, J. W., 1997, Common focus point technology: Ph.D. thesis, Delft University of Technology.